Analytical Modeling and Simulation of the Indoor Radio Propagation Channel

Bulletin of University of Osaka Prefecture
Vol. 44, No. 2, 1995, pp. 69-73

Analytical Modeling and Simulation of the Indoor Radio Propagation Channel

Akifumi HIRATA*, Masanobu KOMINAMI** and Hiroji KUSAKA**

(Received November 30, 1995)

In this paper we propose the indoor wave propagation model combined with the transfer function of multipath reflections. This analysis is based on the moment method and the ray tracing. By means of the moment method, this model can investigate mutual couplings among antennas for diversity effects and cross dipole systems which are difficult to be estimated exactly. The ray tracing enables the model to decide all the imaginary transmitting points against walls. Therefore, this model can be applied to complex structures such as a screen or a board. Furthermore, a practical fading is shown visually and an improvement against concrete deep dips of radio receptive levels is performed easily. In order to confirm the properties of this model, we show wave propagations using circular and linear polarizations and present a comparison of polarized diversity effects between in and out of sight at a L-shape bent corner.

1. Introduction

On purpose of a free wiring, in recent years, wireless LANs in indoor are widely noticed. And it is to be desired that transmission rate of data sequences goes high for wireless communications such as PHS systems and mobile telephones. But multipath reflections from walls or objects in a room compose a stationary wave with deep dips. These dips of an electric field intensity and insufficient frequency bandwidth against high transmission rates result in distortions of a waveform and intersymbol interferences. Particularly in a high-speed data transmission, symbol errors often arise. In this way, the wave propagations of very poor quality have gotten in the way of indoor wireless LANs.

As a scheme to improve the fast fading condition, therefore, the method using diversity antenna systems is well known. Diversity techniques have long been considered a good method for overcoming periodic burst errors caused by deep dips of an envelope level and by fast phase transitions[1]. Moreover, spread spectrum is a strong communication system against these fading transmission channel. Many research papers about it are published actively[2].

In order to construct more effective indoor wireless LANs, it is important to confirm the wave propagation characteristics. Therefore, previous studies have taken statistical methods using mean and variance of delay times[3], and have derived characteristics from some fading models such as Rayleigh fading[4].

On the other hand, in our present work, multipath reflections are treated by the geometric ray tracing deciding all the imaginary transmitting antennas against walls. And the analysis is carried out by deriving a matrix for the amplitude of induced voltage on a receiving antenna. The voltage matrix is derived by using the moment method solution with the Green's function.

Numerical examples using this model are demonstrated in Section 3. An expression of multipath fading in indoor is enforced by illustrating visually deep dips of radio receptive level. There we compare wave propagations using circular and linear polarizations. Also we show the polarized diversity improvements in and out of sight of a L-shape room.

2. Analytical Modeling

The indoor propagation model is shown in Fig. 1. It is remarkable that this analytical model enables the generation of practical fading. The positions of deep dips in fading environments are dependent on the definition of indoor structures and antenna configura-

* Graduate Student, Department of Electrical and Electronic Systems, College of Engineering.
** Department of Electrical and Electronic Systems, College of Engineering.

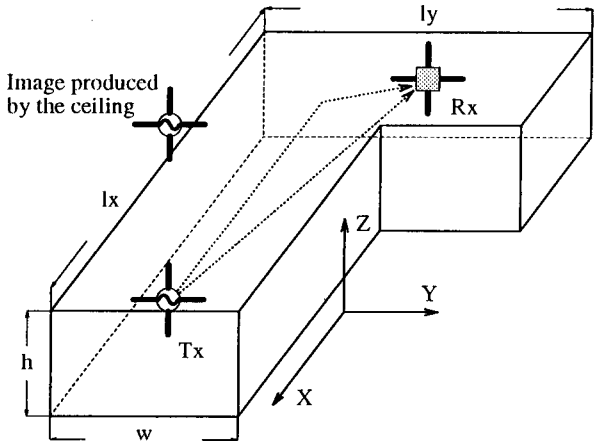

Fig. 1 Indoor wave propagation model

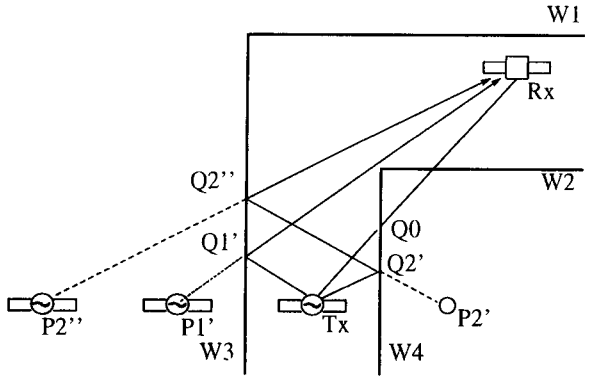

Fig. 2 Interference of the 1 st-order reflective wave on a flat floor.

tions. Though this model is a passage with a bent corner, of course, it is also able to construct other structures such as a columned tunnel.

2.1 Geometric Ray Tracing

In this model, to keep the model as simple as possible, all walls are assumed to be perfect conductor. So multipath reflections are regarded as waves from the antenna's images against walls. All positions of the antenna's images can be found by approaching the geometric ray tracing[5]. This ray tracing is to trace rays geometrically while repeating decisions whether a wall exists or not between a receiving point and an imaginary transmitting one until the defined maximal number of reflection. Therefore, even if a tested room has a shadow fading due to complex structures such as a window or a board, this model can be applied.

For example, in Fig. 2 we explain the algorithm of the ray tracing for a L-shape tunnel structure. For convenience, we assume that diffractions don't exist. The direct wave between the transmitting point Tx and the receiving point Rx doesn't exist, because the path is interfered by the wall W 4. About 1 st-order, we get the imaginary point P 1' of Tx against W 3 and decide the existence of a reflection point Q 1' on wall W 3 between Rx and P 1'. Moreover we decide the existence of an interfering wall between Tx and Q 1' and between Rx and Q 1'. In this case, we decide that the 1 st-order reflection path (Tx-Q 1'-Rx) exists. Similarly, about higher-order reflections we repeat this decision procedure.

2.2 Numerical Theory

As for calculations, since the current distribution on a dipole is approximated by the piecewise sinusoidal (PWS) function, we need to divide all the antennas into a number of small segments. Mutual couplings between these all segments are expressed by a set of simultaneous integral equations. In order to contain these integral equations for antennas into a matrix, we use the moment method solution with the Green's function[6].

This moment method can estimate mutual couplings exactly, for example, for the cases of some diversity systems with adjacent receiving antennas or for the cases where antennas are near to a wall. It has been said that these cases were difficult to analyze by means of a simulation before.

First of all, if the number of the divided segments on all dipoles is N, the unknown current distribution $\boldsymbol{I}(\boldsymbol{r}')$ is expressed in a set of N basis functions of Eq. (1):

$$\boldsymbol{I}(\boldsymbol{r}')=\sum_{n=1}^{N} I_n \boldsymbol{J}_n(\boldsymbol{r}'), \tag{1}$$

where $\boldsymbol{J}_n(\boldsymbol{r}')$ $(n=1, 2, ..., N)$ is the n-th PWS function and I_n is its unknown amplitude, an expansion coefficient.

Next, by boundary conditions at the surface of a dipole, an induced electric field $\boldsymbol{E}(\boldsymbol{r})$ at an observation point $\boldsymbol{r}$ by a source current $\boldsymbol{I}(\boldsymbol{r}')$ and an impressed electric field $\boldsymbol{E}_i(\boldsymbol{r})$ are related by this Richmond's reaction integral equation.

$$\boldsymbol{E}(\boldsymbol{r})+\boldsymbol{E}_i(\boldsymbol{r})\Big|_{\tan}=0 \tag{2}$$

Using Eq. (2), the current distribution on each segment is represented as the following integral equations:

$$\sum_{n=1}^{N} I_n \iint_{S'n} \overline{\overline{\boldsymbol{G}}}(\boldsymbol{r}_m, \boldsymbol{r}'_n)\cdot \boldsymbol{J}_n(\boldsymbol{r}'_n)\, dS'_n = -\boldsymbol{E}_i(\boldsymbol{r}_m), \tag{3}$$

where $\overline{\overline{\boldsymbol{G}}}(\boldsymbol{r}_m, \boldsymbol{r}'_n)$ is the dyadic Green's function between an observation point $\boldsymbol{r}_m$ and a source point $\boldsymbol{r}'_n$ calculated on antennas. The effects of all walls

are contained in $\overline{\overline{G}}(\boldsymbol{r}_m, \boldsymbol{r}'_n)$.

$$\overline{\overline{G}}(\boldsymbol{r}_m, \boldsymbol{r}'_n)=(\nabla\nabla+k^2\overline{\overline{I}})\,\varphi(\boldsymbol{r}_m, \boldsymbol{r}'_n) \tag{4}$$

$$\varphi(\boldsymbol{r}_m, \boldsymbol{r}'_n)=\frac{e^{-jk|\boldsymbol{r}_m-\boldsymbol{r}'_n|}}{|\boldsymbol{r}_m-\boldsymbol{r}'_n|} \tag{5}$$

In order to solve the unknown coefficients I_n, we transform Eq. (3) to a matrix equation (6) by means of the Galerkin's method, which multiplies a weighting function $\boldsymbol{J}_m(\boldsymbol{r}_m)$ same as the basis function $\boldsymbol{J}_n(\boldsymbol{r}_n)$ to both sides of Eq. (3).

$$\sum_{n=1}^{N} Z_{nm}I_n=V_m \qquad (m=1, 2, \cdots\cdots, N) \tag{6}$$

$$[Z]\ [I]=[V] \tag{7}$$

$$[I]=[Z]^{-1}[V] \tag{8}$$

In this case, Z_{nm} and V_m are substituted for the integral components with the Green's function $\overline{\overline{G}}(\boldsymbol{r}_m, \boldsymbol{r}'_n)$ in Eq. (3)

$$Z_{nm}=\iint_{Sm}\iint_{S'n}\boldsymbol{J}_m(\boldsymbol{r}_m)\cdot\overline{\overline{G}}(\boldsymbol{r}_m, \boldsymbol{r}'_n)\cdot\boldsymbol{J}_n(\boldsymbol{r}'_n)\,dS'_n dS_m \tag{9}$$

$$V_m=-\iint_{S_m}\boldsymbol{J}_m(\boldsymbol{r}_m)\cdot\boldsymbol{E}_i(\boldsymbol{r}_m)dS_m \tag{10}$$

By this numerical means, the actual current distribution at all dipoles are presented. And once the current is known, we can determine the electric field intensity in a tested room structure.

3. Numerical Examples and Discussion

Our paper has proposed the indoor wave propagation model. This model's properties are demonstrated in the following figures.

Figures 3 (a) and 3 (b) make a comparison between linear and circular polarizations. It has been reported that the circularly polarized wave is suitable for indoor wireless communications because the odd-order reflection waves change to the reverse rotation. The circularly polarized wave is generated by a set of a half wavelength cross dipole fed with a $\pi/2$ phase shift. Then, the received current I is expressed as

$$\begin{aligned} I&=I_{RV}+I_{RH}\cdot e^{\pm j\frac{\pi}{2}}\\ &=I_{TV0}+I_{TV1}\pm j\,(I_{TH0}+I_{TH1})\\ &=I_{TV0}+I_{TV1}\pm j\,(\mp jI_{TV0}\pm jI_{TV1})\\ &=I_{TV0}+I_{TV1}+I_{TV0}-I_{TV1}\\ &=I_{TV0}\times 2, \end{aligned} \tag{11}$$

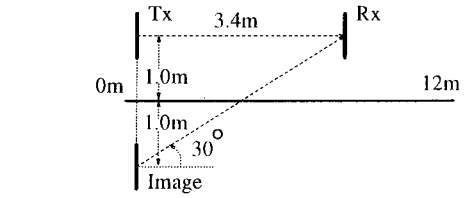

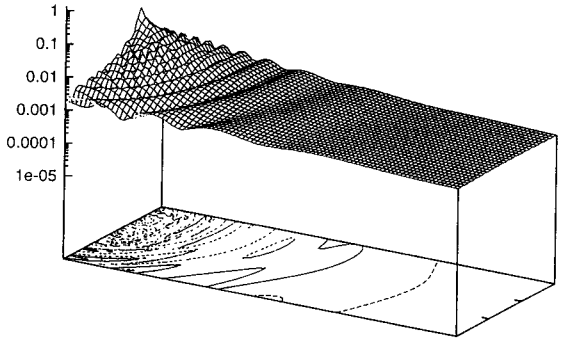

(a) Circularly polarized wave

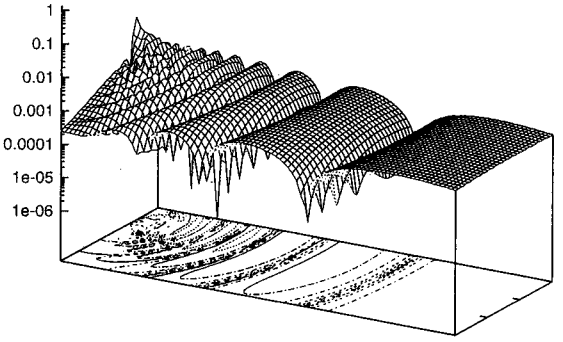

(b) Linearly polarized wave

Fig. 3 Geometric ray tracing.

where I_{TV0}, I_{TH0}, I_{TV1} I_{TH1} indicate directly vertical, directly horizontal, 1 st-order vertical and 1 st-order horizontal components, respectively. Equation (11) proves that the odd-order reflection waves are not acceptable. We adopt 2.4 GHz of the frequency in the ISM band. And the length and the radius of antennas are fixed a half wavelength and a hundred of the length.

In Fig. 3 (a) the vertical dipole and the horizontal dipole of a cross dipole are parallel to the y-axis, and the z-axis, respectively. In Fig. 3 (b) the dipole is parallel to the y-axis. Both transmitting and receiving antennas are located at 1.0 m height above a flat floor.

As the appreciation of this model, when the transmitting antenna is fed with 1.0 V, the induced voltage levels on the receiving antenna in each point of the room are drawn by means of the contour line of equal level distribution.

The directivity of circularly polarized waves using a simple cross dipole have been reported to be about 30°

wide at most from the maximum radiative direction[7]. Because the difference of height between the imaginary transmitting point and the original one is 2.0 m, it is expected about 3.4 m away ($\sqrt{3}$ times the difference) that the wave of the imaginary transmitting point can be received as a circularly polarized wave. In Fig. 3 (a), it is also confirmed that as the receiving point moves away from 3.4 m, the interference of the reflection fades away. On the other hand, deep dips due to the interference appear regularly in Fig. 3 (b). It has the same conditions as Fig. 3 (a).

Moreover, hard oscillations are observed at near x= 3.4 m above the floor in Fig. 3 (a), which is why the redio wave from the original transmitting antenna is received as linearly polarized, not as circularly polarized.

The next Fig. 4 (a) illustrates the polarized diversity effects and the circular polalization, comparing in and out of sight. Fig. 4 (b) shows the vertical and the horizontal polarized reception separately. The reflection order is the first to get concise analytical results. The defined room has a passage with a bent corner of lx=12.0 m, ly=8.0 m, h=3.0 m, w=4.0 m long as in Fig. 1. Same as the former examples, all of the walls consist of perfect conductor and both of the two antennas are located at 1.0 m above the floor. The transmitting antenna is fixed at x=10.0 m, y=2.0 m and the receiving antenna is moving from y=0.125 m through y=7.875 m at the point of x=1.0 m; therefore the receiver goes out of sight from y=5.0 m away. And from about y=5.6 m away, only one radio wave can reach the receiver.

In Fig. 4 (a), in sight the positions of dips for two ways of the reception shift to a half period, while out

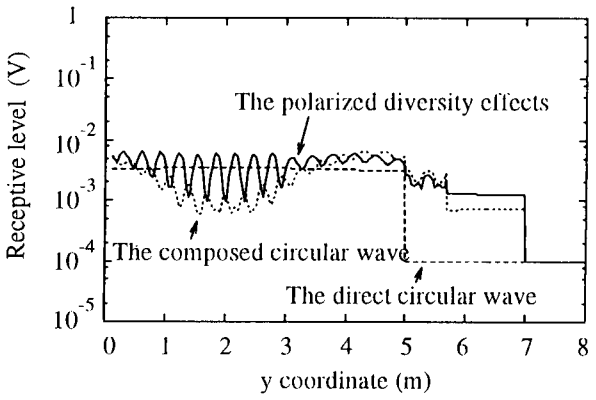

(a) Diversity effects

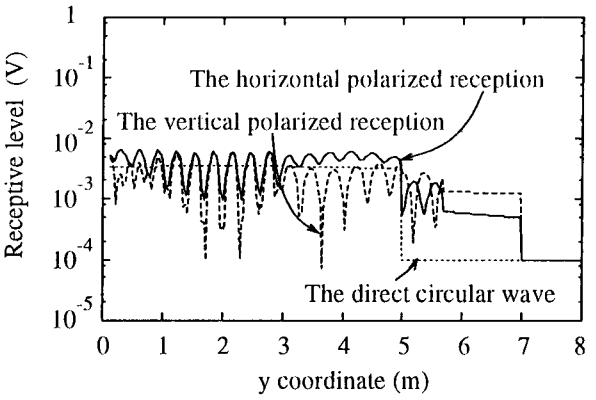

(b) Vertical and horizontal polarizations

Fig. 4 A comparison between in and out of sight. The reflection order is only the first. A passage with a bent corner as in Fig. 1; lx=12.0 m, ly=8.0 m, h=3.0 m, w=4.0 m. The height of both antennas is 1.0 m above on the floor.

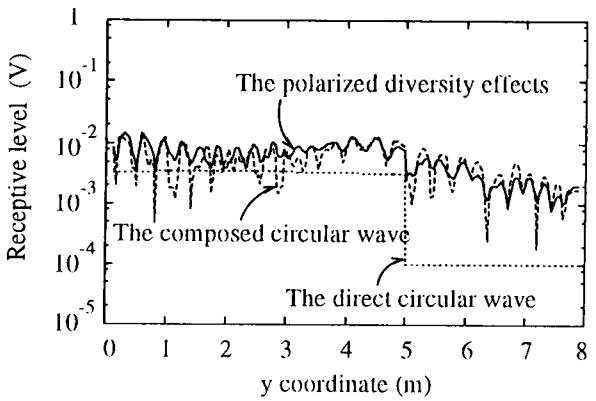

(a) Diversity effects

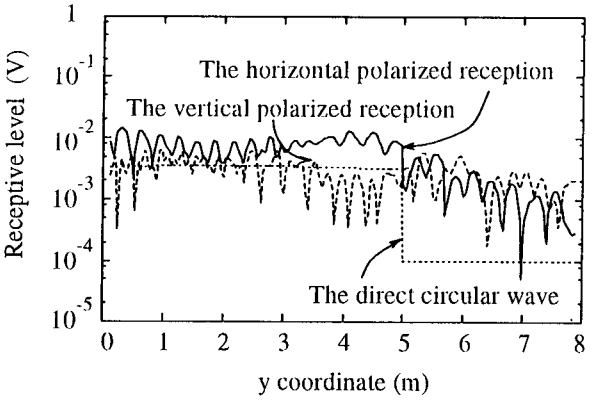

(b) Vertical and horizontal polarizations

Fig. 5 A comparison between in and out of sight. The reflection order is the second. A passage with a bent corner as in Fig. 1; lx=12.0 m, ly=8.0 m, h= 3.0 m, w=4.0 m. The height of both antennas is 1.0 m above on the floor.

of sight the dips are at the same position. The cause of this behavior is thought that out of sight the circularly polarized wave is received as linear polarization. Besides, the total level of the composed circular polarized wave is attenuated as the receiver is near y= 2.0 m, where this receiver faces the transmitting antenna. This is expected because the waves from the transmitting antenna and the ones from other frontal imaginary antennas cancel each other.

To the contrary, in Fig. 4 (b), out of sight the deep dips of the vertical and the horizontal components correlate inversely each other. And in sight the vertical components are interfered intensely because the height of both of the antennas is equal.

Next we have prepared the figure to obtain numerical results of the higher-order reflection waves. This includes the 2 nd-order reflection waves in addition. This example also shows that out of sight two components are good diversity branches.

4. Conclusion

We have proposed the indoor wave propagation model using the ray tracing and the moment method. Since the moment method properly accounts for the mutual coupling among antennas, we can analyze visually the fading environments in circularly polarized wave propagations and research the effects of diversity in and out of sight in the defined room.

We have found out that the composed circular polarized wave may be attenuated at the position where the original cross dipole faces other frontal imaginary ones, though deep dips as observed for a linear polarized wave are reduced. And we have confirmed that in and out of sight the vertical and the horizontal antennas work as good diversity branches. This model can derive a good effective condition of transmission power as low as possible in the tested room.

References

1) S. Sampei, IEICE Trans., Vol. 73, No. 8, August 1990.
2) E. A. Geraniotis and M. B. Pursley, IEEE Trans. Commun., Vol. COM-30, pp. 985-995, May 1982.
3) S. A. Fechtel, IEEE Journal Commun, Vol. 11, No. 3, April 1993.
4) J. G. Proakis, "Digital Communications", MaGraw-Hill Book, New York 1989.
5) J. W. McKown and R. L. Hamilton, Jr, IEEE Network Magazine, pp. 27-30, November 1991.
6) W. L. Stutzman and G. A. Thiele, "Antenna Theory and Design", John Wiley & Sons, pp. 306-371, 1981.
7) Y. T. Lo and S. W. Lee, "Antenna Handbook I", Van Nostrand Reinhold, New York.